OPEN ACCESS
CellPress

Cell Reports
Resource

Path to the Clinic: Assessment of iPSC-Based Cell Therapies In Vivo in a Nonhuman Primate Model

So Gun Hong,[1,5] Thomas Winkler,[1,5] Chuanfeng Wu,[1] Vicky Guo,[1] Stefania Pittaluga,[2] Alina Nicolae,[2] Robert E. Donahue,[1] Mark E. Metzger,[1] Sandra D. Price,[1] Naoya Uchida,[3] Sergei A. Kuznetsov,[4] Tina Kilts,[4] Li Li,[4] Pamela G. Robey,[4] and Cynthia E. Dunbar[1,*]

[1]Hematology Branch, National Heart, Lung and Blood Institute, National Institutes of Health, Bethesda, MD 20892, USA
[2]Laboratory of Pathology, Center for Cancer Research, National Cancer Institute, National Institutes of Health, Bethesda, MD 20892, USA
[3]Molecular and Clinical Hematology Branch, National Heart Lung and Blood Institute-National Institute of Diabetes and Digestive and Kidney Diseases, National Institutes of Health, Bethesda, MD 20892, USA
[4]Craniofacial and Skeletal Diseases Branch, National Institute of Dental and Craniofacial Research, National Institutes of Health, Bethesda, MD 20892, USA
[5]Co-first author
*Correspondence: dunbarc@nhlbi.nih.gov
http://dx.doi.org/10.1016/j.celrep.2014.04.019

SUMMARY

Induced pluripotent stem cell (iPSC)-based cell therapies have great potential for regenerative medicine but are also potentially associated with tumorigenic risks. Current rodent models are not optimal predictors of efficiency and safety for clinical application. Therefore, we developed a clinically relevant nonhuman primate model to assess the tumorigenic potential and in vivo efficacy of both undifferentiated and differentiated iPSCs in autologous settings without immunosuppression. Undifferentiated autologous iPSCs indeed form mature teratomas in a dose-dependent manner. However, tumor formation is accompanied by an inflammatory reaction. On the other hand, iPSC-derived mesodermal stromal-like cells form new bone in vivo without any evidence of teratoma formation. We therefore show in a large animal model that closely resembles human physiology that undifferentiated autologous iPSCs form teratomas, and that iPSC-derived progenitor cells can give rise to a functional tissue in vivo.

INTRODUCTION

The discovery of reprogramming methods able to generate pluripotent cells from adult somatic tissues have stimulated excitement that personalized cell-based regenerative medicine therapies are within reach. Although many proof-of-principle reports support the potential of using tissues produced from induced pluripotent stem cells (iPSCs) for therapeutic purposes, the actual feasibility and safety of these modalities for human clinical applications remains controversial, given very limited relevant preclinical data (de Almeida et al., 2013; Kaneko and Yamanaka, 2013). Most in vivo models for safety or efficacy have studied the behavior of murine iPSC-derived cells in mice, or human iPSC-derived cells in profoundly immunocompromised mice. Although murine models may provide valuable proof-of-principle and mechanistic information, murine physiology substantially differs from the human setting, particularly in regard to the immune and inflammatory systems (Seok et al., 2013). There appear to be quite significant differences between murine and human iPSCs or embryonic stem cells (ESCs) even when profiled in vitro (Tesar et al., 2007). Human cells implanted in immunodeficient mice are unlikely to be able to integrate normally into appropriate niches or assessed functionally, and any interaction between human iPSCs and the immune system cannot be addressed.

The teratoma assay has been the gold standard by which to document pluripotency of human pluripotent stem cells (PSCs) (Cunningham et al., 2012), but also assumes a preclinical importance to assess whether any pluripotent, tumorigenic cells remain in the cell population following its differentiation into a therapeutically relevant tissue of interest. Therefore, development of an autologous preclinical teratoma model is desirable. Recently, Zhao et al. reported that murine iPSCs were more immunogenic than murine ESCs and could elicit T cell-mediated immune responses against several teratoma proteins in syngenic immunocompetent mice (Zhao et al., 2011). However, two subsequent papers reported no immune rejection of murine iPSC or their differentiated progeny tissues in syngenic mice (Araki et al., 2013; Guha et al., 2013). These conflicting results, in addition to the inherent limitations of rodent models for modeling the physiology, safety, and efficacy of novel therapies, have prompted us to develop a relevant large animal preclinical model for iPSC therapies.

The rhesus macaque has been a very valuable model organism for development of novel cell and gene therapies, and analysis of the immune system. Physiological similarity including size and life span, phylogenetic similarity to humans, cross-reactivity of human cytokines and antibodies, completed genome sequencing, and knowledge gained from 3 decades of macaque immunologic studies stimulated by the HIV epidemic contribute to the utility of this model (Donahue and Dunbar, 2001; Lackner and Veazey, 2007). Moreover, rhesus iPSCs resemble human

iPSCs in terms of morphology, marker expression, and growth factor dependency to maintain their pluripotency (Liu et al., 2008).

Bone regeneration is needed in case of critical bone defects due to trauma, surgical resection of tumor, infection, aseptic loosening of prosthetics, or nonunions (Steinert et al., 2012). Bone marrow stromal cells (BMSCs), also termed mesenchymal stromal cells or mesenchymal stem cells (MSCs), can be differentiated toward the osteogenic lineage and used to create new osteoid matrices and new bone (Quarto et al., 2001; Robey, 2011). Therefore, substantial research efforts in the field of orthopedic regenerative medicine have been devoted toward developing specific cell-based osteogenic therapies using BMSCs. Although BMSCs can be isolated from adult tissue, the procedure is invasive, expensive, and laborious. Furthermore, adult BMSCs may have a limited expansion capacity in vitro, especially when obtained from aged donors and therefore may not be suitable to generate sufficient therapeutic cells (Illich et al., 2011; Roobrouck et al., 2008). iPSCs could serve as a virtually unlimited autologous source of osteogenic precursor cells; in addition, genetically corrected BMSCs can potentially be used for treatment of genetic bone diseases. We target this mature tissue as a proof of principle for autologous tissue regeneration from iPSCs in a relevant large animal model.

RESULTS

Derivation of Transgene-free Rhesus iPSCs and Adaptation to a Xeno-free Culture Surface

Rhesus iPSCs were generated via reprogramming of rhesus BMSCs (RhBMSCs), skin fibroblasts, or $CD34^+$ cells with the excisable polycistronic lentiviral vector, STEMCCA, expressing human *POU5F1* (*OCT4*), *SOX2*, *MYC*, and *KLF4* (Sommer et al., 2010). Some rhesus dermal fibroblasts were transduced with the inducible caspase-9 (iCasp9) suicide gene (Di Stasi et al., 2011) before reprogramming. Rhesus iPSCs were documented as pluripotent by morphology, gene expression, in vitro differentiation, and teratoma formation in immune-deficient NOD scid gamma c (NSG, NOD.Cg-Prkdcscid Il2rgtm1Wjl/SzJ) mice (Figure S1). The transgene cassettes were excised by transient expression of Cre recombinase (Merling et al., 2013). Excision was confirmed by PCR (Figure 1A) and Southern blot (data not shown). Five transgene-free rhesus iPSCs (RhiPSCs) clones from two animals were selected for further experiments (Table S1). These clones had normal and stable karyotypes, with G-banding repeated just prior to selected in vivo autologous implantation experiments. The genomic location of the 303 bp nonexpressed proviral vector fragment remaining in the genome following the transgene-excision was mapped by a modified restriction enzyme-free linear amplification-mediated polymerase chain reaction (Re-free LAM-PCR) (Wu et al., 2013) in the RhiPSC clones to be used for autologous transplantation (Table S1). The presence of this inert DNA tag allowed unequivocal assessment of the presence or absence of RhiPSCs following in vivo implantation. Rhesus ESCs (RhESCs, ORMES-22) (Mitalipov et al., 2006) were used as a positive control in all in vitro iPSC characterization steps, including teratoma formation in immunodeficient mice (Figure S1).

Transplantation of iPSCs or their progeny into an immunocompetent recipient in a clinical setting requires feeder-free, and ideally, completely xenogeneic-free defined cell culture conditions. We successfully adapted RhiPSCs to feeder-free cultures using the widely used murine basement membrane tumor extract, Matrigel, or Synthemax II-SC, a chemically defined animal-free surface coating. Under these conditions, the RhiPSCs retained ESC-like morphology, normal karyotype, and their pluripotent phenotype as demonstrated by expression of typical pluripotent markers such as OCT4, NANOG, SSEA4, TRA-1-60, differentiation in vitro into embryoid bodies (EBs) comprising the three embryonic germ layers, and teratoma formation in NSG mice (Figures 1B–1K). Table S1 summarizes characterization results for the five RhiPSC clones used in subsequent in vivo and in vitro studies of teratoma formation and differentiation.

Development of a Xeno-free Teratoma Assay

Extracellular matrix protein has been shown to greatly enhance teratoma formation of PSC in the xenograft setting, particularly with subcutaneous cell implantation approaches (Prokhorova et al., 2009). Alternative injection methods such as intratesticular, intramuscular, or renal subcapsular injections are not practical and are too invasive to permit repeated harvesting in a nonhuman primate transplant model. Use of subcutaneous injection also permitted more injections per animal and allowed continuous monitoring of mass size via calipers or ultrasound, without repeated invasive procedures or prolonged anesthesia, and permitted retrieval of the implants at various time points for analysis, without danger to the animal. However, the most commonly used supportive compound, Matrigel is composed of proteins secreted by the murine Engelbreth-Holm-Swarm sarcoma and is therefore likely to be highly immunogenic following injection into an immune competent host such as the rhesus macaque. We therefore tested alternative approaches for teratoma assays in NSG mice. We hypothesized that use of an autologous rhesus macaque three-dimensional matrix would be most physiologic and relevant, and thus we tested if a rhesus macaque plasma clot scaffold could be substituted for Matrigel in teratoma assays.

The kinetics and quality of subcutaneous teratoma formation in NSG mice from RhiPSCs suspended in a rhesus plasma clot was comparable to those of teratoma formation in NSG mice using Matrigel scaffold (Figure S2). The subcutaneous injection of RhiPSCs suspended in IMDM medium alone, without any three-dimensional matrix, was not sufficient to support teratoma formation.

Autologous Teratoma Formation in the Rhesus Macaque

Utilizing the plasma clot method, we tested whether or not autologous iPSCs form teratomas in vivo in immunecompetent rhesus macaques. A range of cell doses for three independent Cre-mediated transgene excised autologous RhiPSC clones (5×10^5–5×10^6 cells) were suspended in an autologous clot and injected subcutaneously into the original #ZG15 donor macaque at a total of six sites (first teratoma assay).

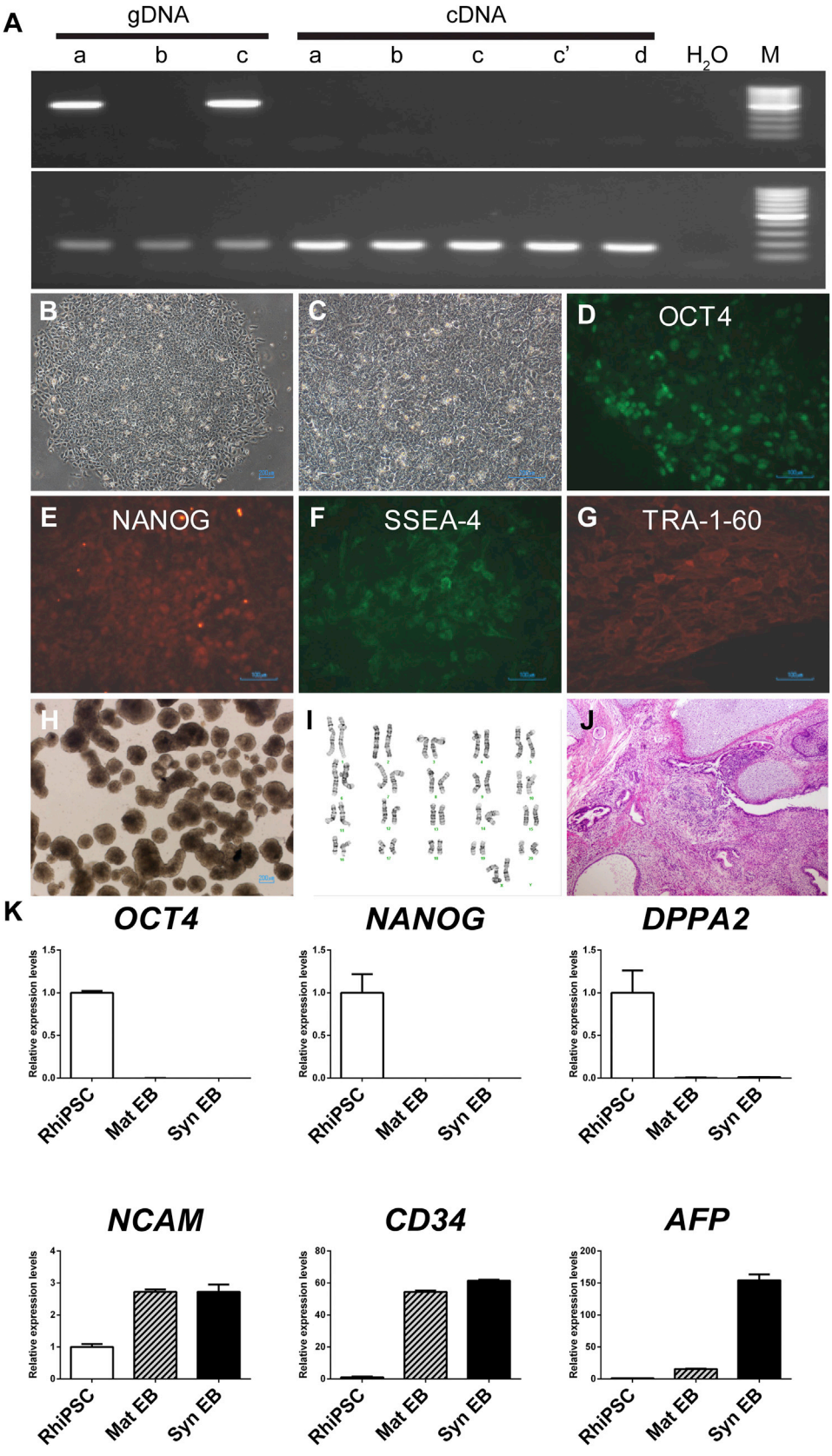

(legend on next page)

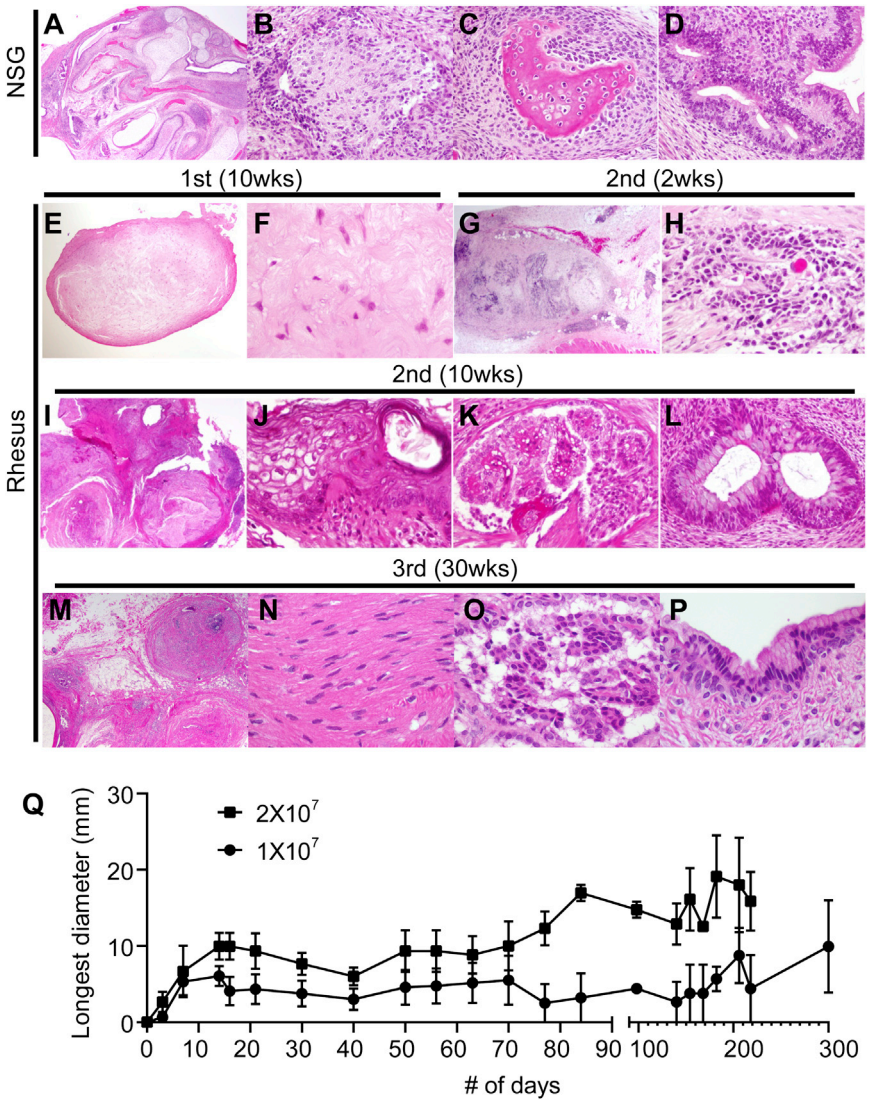

Figure 2. Autologous Teratoma Assay in Rhesus Macaques

(A–D) All RhiPSCs in autologous plasma clots formed teratomas in NSG mice. Histologically, the tumors showed tissues derived from all three germ cell layers (A, H&E 20×) including immature (rare foci) and mature neuroepithelial elements (B, H&E 200×), bone (C, H&E 200×) and cartilage (A), and glandular structures (D, H&E 200×).

(E and F) In the first autologous rhesus macaque experiment, one out of six implants of 1×10^5 RhiPSCs formed a well-defined 5 mm nodule, and the mass was harvested at 10 weeks. On H&E staining, dense, fibrous connective tissue with no evidence of teratoma formation was observed (E, H&E 20×; F, H&E 400×).

(G and H) When 1×10^7 RhiPSCs were injected autologously (second teratoma assay), an immature teratoma developed 2 weeks post-injection. The well-circumscribed nodule (G, H&E 20×) showed proliferating immature neuroepithelial cells with scattered rosette formation (H, H&E 400×).

(I–L) A mature teratoma developed by 10 weeks after 1×10^7 RhiPSCs implantation, consisting of mature glial tissue (I, H&E 20×), squamous epithelium (J, H&E 400×), well-vascularized papillary choroid plexus structures (K, H&E 200×), and well-differentiated glandular epithelium with goblet cells (L, H&E 200×).

(M–P) The 30 week RhiPSCs-derived masses (M, H&E 20×, third teratoma assay) showed structures consistent with peripheral nerves (N, H&E400×), choroid plexus (O, H&E 400×), and mucinous epithelium (P, H&E 400×).

(Q) Growth kinetics of RhiPSC-derived mass size per delivered cell number in autologous rhesus macaques. Six 1×10^7 RhiPSC-derived masses and three 2×10^7 masses were measured using ultrasound every 7–10 days up to day 100. From days 101 to 300, there were only two tumors available for follow-up per each cell concentration. Values represent mean ± SEM. See also Figures S2 and S3.

Concurrently, the same cells and clot preparations were injected subcutaneously into NSG mice. In this initial experiment, the RhiPSCs had been adapted to feeder-free growth on Matrigel and were washed extensively to remove residual Matrigel before suspension in plasma for injection. All animals were closely monitored for teratoma formation, with up to 21 months of follow-up.

By 7 weeks, all NSG mice developed mature teratomas of greater than ~2 cm diameter (Figures 2A–2D). In contrast, only one of six injection sites in the macaque had a palpable tumor,

Figure 1. Feeder-free Culture of Transgene-free Rhesus iPSCs

(A) Transgene excision and silencing was documented by PCR and RT-PCR. (a, RhiPSC clone pre-excision; b, RhiPSC clone postexcision; c and c′, RhiPSC (pre-excision)-derived SCs, p4 and p12, respectively; d, BMSCs.) Upper panel: *MYC/WPRE*; lower panel: *ACTIN*.

(B–G) A long-term feeder-free culture of RhiPSCs was successful on both Matrigel-coated (Mat) and Synthemax II-SC-coated (Syn) plates. These cells retained typical ESC morphology (B, 40×; C, 100×) and expressed pluripotency proteins, OCT4 (D, 200×), NANOG (E, 200×), SSEA-4 (F, 200×), and TRA-1-60 (G, 200×).

(H) RhiPSCs cultured on both Mat and Syn were able to differentiate into embryoid bodies (EBs) (40×).

(I and J) They maintained normal karyotype (I) and were able to form teratomas in NSG mice, with derivates from all three germ cell layers including glandular elements, cartilage, and neuroepithelial cells (J, hematoxylin and eosin [H&E] 40×). (B)–(J) show representative figures from clone M22-8 cultured on Synthemax II-SC-coated plates for 1 month.

(K) Differential expression of pluripotent and lineage specific genes following in vitro differentiation using EB method. Gene expression was normalized to undifferentiated RhiPSCs. Values represent mean ± SEM. Mat EB and Syn EB represent mRNA expression from EBs derived from RhiPSCs cultured on Matrigel-coated plates or Synthemax II-SC-coated plates, respectively. See also Figure S1 and Table S1.

Table 1. A Summary of Teratoma Formation Rates from RhiPSCs in Autologous Macaques and NSG Mice

	ZG15						
RhiPSC No.	1st assay	2nd assay	3rd assay	Total	ZG47 (4th assay)	Rhesus Total	NSG
5×10^5	0/2	0/1	—	0/3	0/2	0/5	2/2
2×10^6	0/3	—	—	0/3	0/2	0/5	2/2
5×10^6	0/1	—	—	0/1	—	0/1	—
1×10^7	—	2/3	1/1	3/4	1/6	4/10	3/3
2×10^7	—	—	2/2	2/2	1/2	3/4	2/2

Tumors that were not harvested for PCR, qPCR, and histology analyses were not included in this table. See also Table S2.

a small 2 mm nodule noted 8 weeks after injection (M22-8 iPSC, 5×10^5 cells injected). The nodule size increased to 5 mm by week 9 but then stopped growing and was removed for analysis at 10 weeks. Histologically, the nodule consisted of homogenous, hypocellular fibrocollagenous tissue without evidence of teratoma structures (Figures 2E and 2F). Although the RhiPSCs were extensively washed to remove Matrigel prior to suspension in autologous clot and implantation, we hypothesized that residual Matrigel may have triggered an immune response that inhibited teratoma formation in the immune-competent autologous rhesus macaque.

Therefore, as detailed above, we adapted RhiPSCs to culture on the completely animal-free, synthetic surface Synthemax II-SC, which had been previously determined not to elicit systemic toxicity nor irritation in immune-competent animals (tested by NAMSA). We performed the subsequent autologous teratoma assays using Synthemax II-SC-cultured RhiPSCs (second teratoma assay). We also increased the maximum cell number implanted to 1×10^7 per site. Using cells from ZG15, NSG mice again developed mature teratomas whether low (5×10^5) or high (1×10^7) cell doses were implanted, but 5×10^5 RhiPSCs injected subcutaneously into the autologous ZG15 rhesus macaque exhibited no tumor growth for up to 15 months follow-up (Tables 1 and S2). In contrast, ZG15 sites injected with 1×10^7 RhiPSCs developed palpable masses with the first 7 days postinjection, and these masses slowly increased in size and then plateaued within a 10 week observation period. Tumors were explanted serially at 2, 5, and 10 weeks. Masses harvested at 2 weeks contained immature teratoma structures histologically, mainly consisting of primitive neuroepithelial tissue (Figures 2G and 2H). At 5 weeks, we found fibromyxoid tissue with stellate mesenchymal cells and scattered capillaries, without evidence of ectodermal or endodermal tissue differentiation (Figures S3A and S3B), similar to the fibrous nodule explanted in the first experiment. Samples harvested at 10 weeks had mature structures derived from all three germ cell layers, histologically fulfilling diagnostic criteria for a mature teratoma (Figures 2I–2L). Teratomas persisted out to at least 30 weeks postinjection (third teratoma assay, Figures 2M–2P). In a second animal, ZG47 (fourth teratoma assay), Synthemax II-SC-cultured autologous RhiPSCs formed teratomas with similar kinetics to the first animal, at cell doses of $1–2 \times 10^7$ cells (Figures S3C–S3F). However, sites injected with $5 \times 10^5–2 \times 10^6$ cells did not show any tumor growth. Results of all concurrent rhesus and NSG teratoma assays are summarized in Tables 1 and S2. Figure 2Q summarizes the kinetics of growth for all RhiPSC-derived masses in autologous rhesus macaques.

Conventional and quantitative PCR (qPCR) confirmed that all explanted tissues were of RhiPSC origin, based on the presence of the residual vector DNA 303 bp tag, detected using primers flanking the site of DNA tag insertion or directly targeting internal sequences within the DNA tag (Figure 3). Of note, some tumors consisted only of fibromyxoid tissue and therefore did not fulfill the diagnostic criteria for teratomas (Figures S3A and S3B and Table S2). In summary, we performed autologous teratoma assays using a total of 25 independent undifferentiated iPSC implants in the monkeys, with concurrent comparison to the same cells injected into immunodeficient mice. Nine of nine implants at the cell doses used in this study resulted in teratomas in NSG mice versus seven of 25 in rhesus macaques ($p = 0.0002$ Fisher's exact test), indicating that teratoma formation is less efficient in autologous monkeys than in NSG mice.

Differentiation of RhiPSCs toward Mesodermal Stromal Cells and Development of an Autologous Bone Regeneration Model

Mesodermal stromal cells, also termed BMSCs, are defined by adherent growth on plastic surfaces, typical fibroblastic morphology, and the potential to form skeletal tissues, including bone, cartilage, adipocytes, and hematopoiesis-supporting stroma (Bianco et al., 2001, 2008). Functionally similar cells derived from human iPSCs could potentially be used for tissue replacement, in particular, for osteogenic diseases such as osteogenesis imperfecta (Robey, 2011). We investigated whether RhiPSC-derived mesodermal stromal-like cells (RhiPSC-SCs) could generate viable bone tissue in our autologous nonhuman primate transplant model, in the absence of teratoma formation or other adverse consequences. RhiPSCs were differentiated in BMSC medium supplemented with platelet-derived growth factor AB (PDGF), epidermal growth factor (EGF), and fibroblast growth factor-basic (bFGF) (Figure 4A). Although the stromal-like differentiation efficiency was comparable between RhiPSC clones derived from various somatic cell sources such as fibroblasts, BMSCs or $CD34^+$ cells, we observed some interclonal variation in the efficiency of differentiation to cells with typical connective tissue marker expression. Therefore, we enriched for cells with a stromal-like phenotype via positive immunoselection for the cell surface MSC marker CD73, following 7–10 days in a differentiation culture (Figure S4). This approach yielded a phenotypically and morphologically homogenous

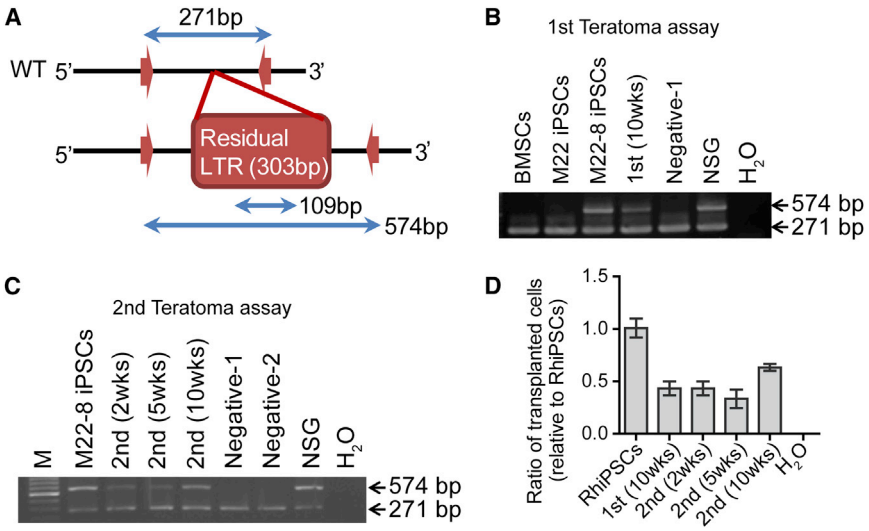

Figure 3. Molecular Analysis to Define the Source of Tissue Masses

(A) PCR strategy to confirm that explanted tumors originated from implanted RhiPSCs (M22-8) is shown. Primers targeting either the residual DNA tag (internal, 109 bp) or the genomic sequence adjacent to the viral integration site (external) were used.

(B and C) Representative insertion-specific PCR utilizing external primers from ZG15 masses harvested at 10 weeks in the first teratoma assay (B) and at 2, 5, and 10 weeks in second teratoma assay (C) are shown. The 271 bp band represents the remaining wild-type allele of the chromosome 3 location and the 574 bp band corresponds to the allele containing the residual vector DNA sequence. M, markers; BMSCs, bone marrow stromal cells; M22, rhesus ZG15 iPSCs before excision; M22-8 iPSCs, transgene-free M22 iPSCs after excision; Negative-1, excised tissue from site injected with plasma clot alone; Negative-2, fat tissue surrounding teratoma mass in ZG15; NSG, M22-8 iPSC-derived teratoma removed from NSG mouse.

(D) Quantitative PCR with internal primers on tumors from first- and second-transplantation harvest after 2, 5, and 10 weeks confirm RhiPSC origin of harvested tissue. Copy numbers are normalized to parental RhiPSC. Values represent mean ± SEM.

population of cells very similar to primary RhBMSCs grown from the bone marrow (Figure 4B), expressing the MSC markers CD44, CD73, CD90, CD105, and CD166 (Figure 4C) but not pluripotency genes (Figure 4D). These differentiated RhiPSC-SCs but not parental RhiPSCs expressed MHC Class I (Figure 4E). RhiPSC-SCs could be further differentiated toward the osteogenic lineage in vitro (Figure 4F) and did not form teratomas in NSG mice followed up to 1 year (Table S3). We also derived mesodermal stromal-like cells from RhESCs, and they were similar to both RhBMSCs and RhiPSC-SCs in terms of gene expression and MSC marker expression (Figure S5).

We initially tested the in vivo osteogenic differentiation potential of autologous bone-marrow-derived RhBMSCs, to document that the bone regeneration model utilizing non-iPSC-derived primary cells was informative in primates. Rhesus macaque primary BMSCs were grown from a marrow aspirate and 2×10^6 cells were mixed with hydroxyl apatite/tricalcium phosphate (HA/TCP) ceramic particles and implanted subcutaneously at multiple sites in the autologous macaque. The transplants were retrieved at 8, 12, and 16 weeks later. Histologically proven bone was formed as early as 8 weeks after implantation (data not shown), similar in structure to bone formed using human BMSCs implanted in immunodeficient mice at early time points (Kuznetsov et al., 1997).

Four independent RhiPSC-SCs derived from the same RhiPSC clones used for the teratoma assays were mixed with HA/TCP particles and implanted subcutaneously at a total of five sites in the autologous macaques. Concurrently, primary autologous RhBMSCs were implanted as comparators, as well as HA/TCP alone, without cell seeding. All grafts derived from RhiPSC-SCs showed robust bone formation at 8 weeks regardless of their RhiPSC origin, such as fibroblasts, BMSCs or $CD34^+$ cells. Histologically, the structures resembled bone tissue derived from RhBMSCs (Figure 5). No bone formation was observed with HA/TCP particles alone. Importantly, no teratoma structures were observed in RhiPSC-SC implants. To investigate whether detectable residual teratoma or tumor-forming cells persist in the differentiated RhiPSC-SC implants and whether bone formation was stable over time, we harvested three independent RhiPSC-SC-derived implants at later time points (27–39 weeks). Again, the implants exhibit robust bone formation with no evidence of teratoma formation (Figure 5).

Characterization of Inflammatory Infiltrates in Autologous Implants

Masses arising from implantation of undifferentiated autologous RhiPSCs of ZG15 and ZG47 showed marked infiltration of inflammatory cells, whereas those cells were absent in the teratomas forming when the same cells were injected into immune-deficient NSG mice. Immunohistochemistry showed mixed B- and T-lymphocytic aggregates, mainly located in the surrounding adipose tissue with some $CD4^+$ and $CD8^+$ lymphocytes scattered within the tumors (Figure 6). Additionally, eosinophils infiltrated the immature teratoma harvested at 2 weeks (Figure 6A). In the organized follicles with germinal centers, as well as a few well-formed granulomas consisting of epithelioid histiocytes admixed with multinucleated giant cells, dominated the inflammatory infiltrates (Figure 6B).

In both autologous BMSC and RhiPSC-SC-derived implants, other than foreign-body giant cells reflecting phagocytized HA/TCP particles, very few small clusters of lymphocytes were present up to 39 weeks of follow-up (Figure S6). Therefore, the cellular inflammatory response was stronger following the implantation of undifferentiated RhiPSCs as compared to the differentiated cell grafts derived from the same RhiPSC clones. Moreover, sites injected with autologous plasma clots with no cells or RhiPSC-SCs, or autologous fibroblasts cultured on Synthemax II-SC in RhiPSCs culture medium and suspended in autologous clot did not evoke inflammation nor tumor formation.

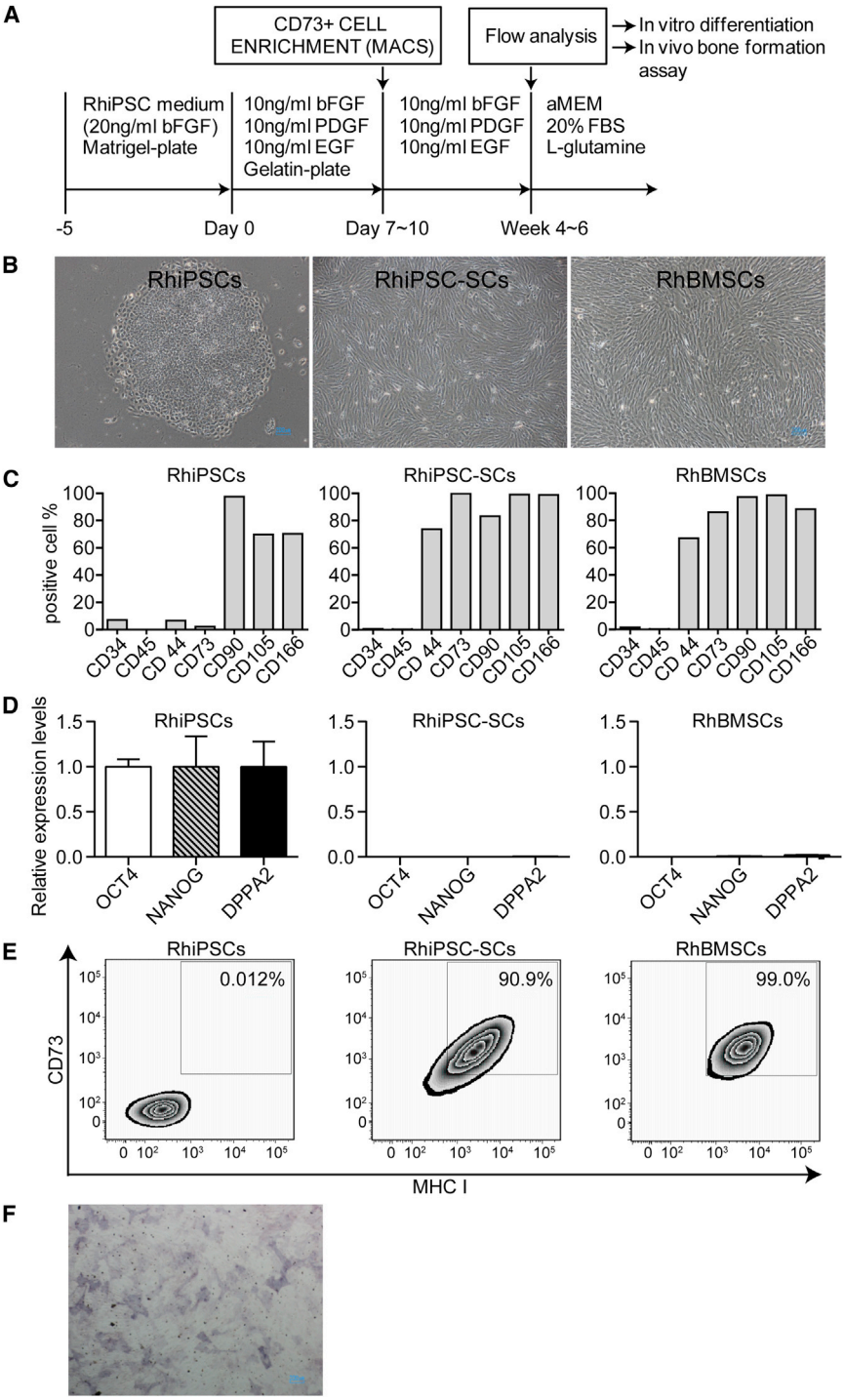

Figure 4. Mesodermal Stromal-like Cells Differentiated from RhiPSCs

(A) Schema for the culture and enrichment steps for RhiPSC-SCs derivation.

(B and C) After 4–6 weeks, RhiPSC-SCs show typical BMSC morphology (B) and express appropriate phenotypic markers as assessed by flow cytometry, comparable to primary RhBMSCs (C).

(D) After differentiation of RhiPSCs toward the mesodermal lineage, pluripotency gene expression was downregulated, as assessed by qPCR. Gene expression was normalized to undifferentiated RhiPSCs. Values represent mean ± SEM.

(E) MHC class I expression was absent on RhiPSCs and upregulated following differentiation to RhiPSC-SCs, with CD73 used as a marker of differentiation toward the mesodermal lineage.

(F) RhiPSC-SCs could be differentiated to osteogenic cells in vitro as demonstrated by alkaline phosphate staining (40×).

(B)–(F) are from a single representative data set. See also Figures S4 and S5 and Table S3.

To investigate whether there is an association between residual endogenous pluripotency gene expression and immunogenicity, immunostaining for OCT4 was performed on tumor masses. No OCT4-positive cells were detected in any autologous teratoma (Figure S7). To investigate whether the inflammatory response persists or has ablated in teratoma tissues over time, masses from the ZG15 monkey were harvested at 30 weeks following implantation. Interestingly, the inflammatory cell collections were still present; however, the teratoma structures remained intact, without evidence for significant tissue damage (Figure 6C). Moreover, plasma cells were present, suggesting chronic inflammation.

DISCUSSION

This study reports the parallel assessment of the tumorigenic potential of undifferentiated iPSCs and the regenerative capacity of iPSC-derived somatic cells in a clinically relevant immune competent model. The risk of residual pluripotent cells forming teratomas or other tumors following transplantation of the tissues derived from iPSC-derived cells is a major concern impacting on future therapeutic applications of iPSC-derived differentiated cells. Strategies to reduce the risk by optimizing differentiation procedures, identifying new PSC-specific selection markers (Tang et al., 2011), inhibitors (Ben-David et al., 2013), or suicide ablation (Zhong et al., 2011) are currently under investigation but require a relevant physiologic model. In particular, preclinical models allowing assessment of the risks associated with the use of autologous iPSC-derived cells in the presence of an intact immune system are critical.

Recent conflicting studies regarding the possible immunogenicity of iPSCs or their differentiated progeny have generated intense interest and require further investigation of this issue in

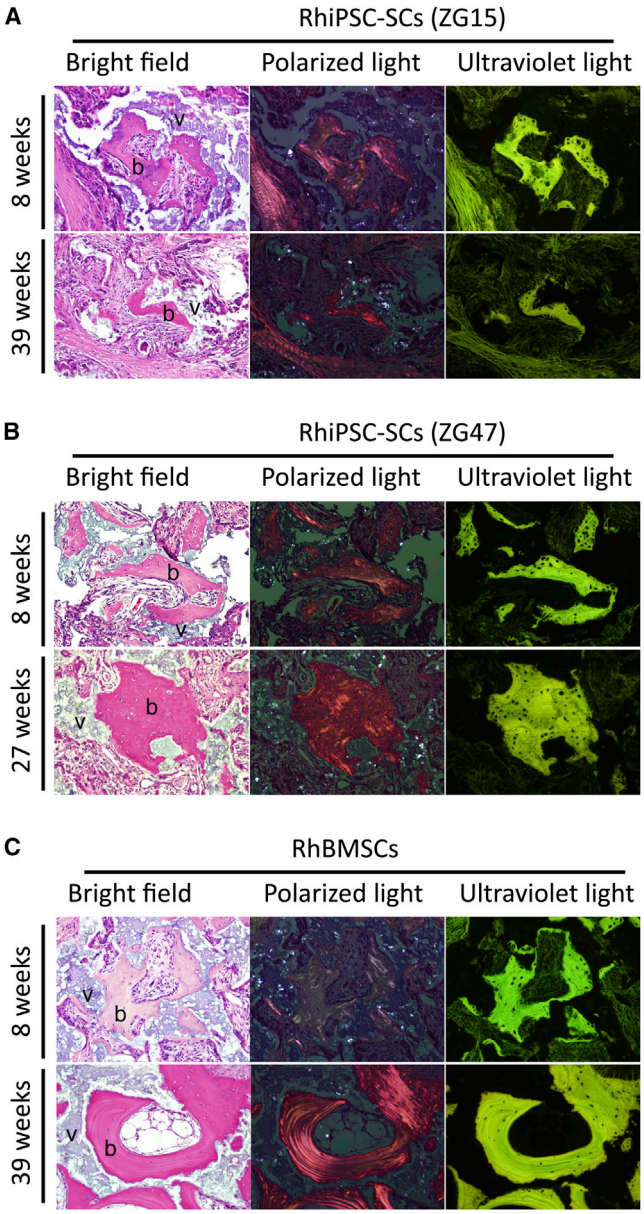

Figure 5. In Vivo Bone Formation from RhiPSCs

RhiPSC-SCs or RhBMSCs mixed with HA/TCP were implanted subcutaneously into the autologous donor animal and harvested at different time points as late as 27–39 weeks postimplantation. H&E-stained slides were analyzed either under bright field, polarized, or ultraviolet light. Multiple foci of new bone formation were present in RhiPSC-SC implants. (A) shows bone in animal ZG15 derived from iPSC clone M11-10 RhiPSC-SCs; (B) shows bone in animal ZG47 derived from iPSC clone H11-4 RhiPSC-SCs, and (C) shows bone in animal ZG15 derived from BMSCs. The irregular bone trabeculae were rimmed by osteoblasts and showed scattered osteocytes. Under polarized light, collagen bundles were observed in bone matrix, organized in parallel patterns consistent with the lamellar structure of new bone. Under ultraviolet light, new bone demonstrated intense green fluorescence consistent with highly mineralized bone matrix. Long-term follow-up (27–39 weeks) of RhiPSC-SC implants demonstrated stable bone formation with no evidence of teratoma formation even this late. b, bone; v, vehicle. Images were taken at 200×.

a model with real relevance to the administration of autologous or HLA-matched human iPSC-derived cells to patients (Araki et al., 2013; Guha et al., 2013; Zhao et al., 2011). Undoubtedly, murine models are valuable proof-of-principle tools for biological and medical research but also have major limitations in predicting more complex physiological processes involving the immune system (Seok et al., 2013) or integration of transplanted cells into functional organs. Furthermore, it is not clear if the phenotypes of murine iPSCs and the molecular pathways maintaining self-renewal are equivalent to those of human or nonhuman primate counterparts (Okita and Yamanaka, 2006; Rao, 2004; Schnerch et al., 2010).

Because of their physiological similarities to humans, nonhuman primates can serve as a valuable translational research model in moving toward early phase clinical trials in humans. Modeling of all steps in iPSCs derivation, characterization, differentiation, and autologous delivery can be accessed via this model. The macaque immune system has been well characterized due to the utility of macaques as models for HIV/AIDS and is highly predictive of the human immune response (Picker et al., 2012). The size and prolonged life expectancy of macaques allow relevant long-term observation with repeated sampling of administered iPSC-derived cells, very difficult in murine models or in a clinical setting. Recently, Emborg et al. reported that autologous rhesus iPSC-derived neuronal cells transplanted intracerebrally showed engraftment ability as well as lack of lymphocyte infiltration (Emborg et al., 2013). However, the CNS is an immunologically protected and unique environment. Therefore, there is still a question about immunogenicity and tumorigenicity of iPSCs and their differentiated derivates when they are grafted into immunocompetent sites (Lee et al., 2013; Tang et al., 2013). Hence, there is a need to assess the safety and efficiency of iPSC-based therapies in a clinically relevant model (Kaneko and Yamanaka, 2013). To our knowledge, there is no prior report of a teratoma assay in a large animal model or a concurrent teratoma and differentiated tissue analysis.

In this study, we developed an autologous teratoma formation assay in the rhesus macaque, following a long process of optimization in vitro and in vivo, removing xenogeneic components such as Matrigel from the culture surface and implantation scaffolds because it will likely trigger rejection of the RhiPSCs or their progeny in an immunocompetent organism. Removal of xenogeneic components is also highly desirable from a regulatory standpoint. We found that the Matrigel scaffold could be replaced by an autologous plasma clot to reaggregate and support RhiPSCs implanted in vivo, as shown previously for implanted neural cells (Lindsay et al., 1987). Besides the three-dimensional scaffold function, plasma may also support teratoma formation by providing growth factors stimulating both iPSCs themselves, as well as angiogenesis required for teratoma or other new tissue growth. Using this assay, we were able to show that undifferentiated iPSCs can indeed form teratomas in vivo. This method is simple and noninvasive and can be used for a variety of applications in the investigation and clinical development of tissue regenerative therapies. Up to 30 sites can be injected and harvested in a single macaque, without evident discomfort or clinical complications.

In this context, it is noteworthy that although the autologous RhiPSCs did form mature teratomas in the macaques, the

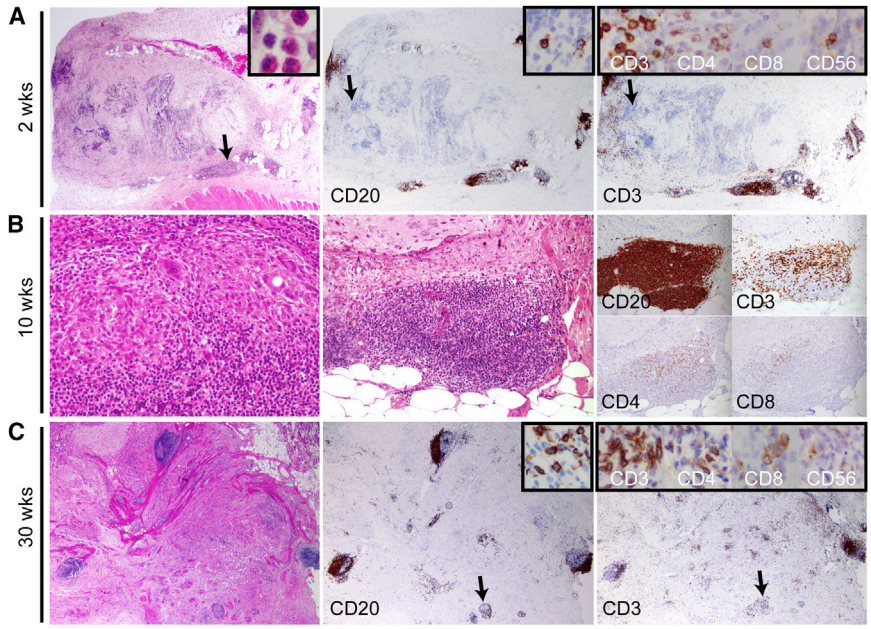

Figure 6. Inflammatory Reactions at RhiPSCs Autologous Rhesus Macaque Injection Sites

(A) Inflammatory reactions at 2 weeks in the second teratoma assay. The mass shows multiple lymphoid aggregates in the surrounding adipose tissue (left panel) together with numerous eosinophils (detail inset 1,000×). The arrow in the original picture indicates the location of the detail inset. Immunostaining shows both CD20-positive B cells (middle panel, detail inset 400×) and CD3-positive T cells (right panel). Among T cells, CD4-positive cells and a few CD8-positive cells were present. A few scattered CD56-positive NK cells are also found. High-power pictures of CD3, CD4, CD8, and CD56 are shown in insets of CD3 (all 400×).

(B) Inflammatory reactions at 10 weeks in the second teratoma assay. The 10 week teratoma was associated with granulomas consisting of epithelioid histiocytes admixed with multinucleated giant cells (left panel, 200×) as well as mature lymphoid follicles with well-formed germinal centers (middle panel, 200×). Immunostaining of the germinal center with CD20, CD3, CD4, and CD8 is shown in (B), right panel (all 200×).

(C) Inflammatory reactions in the long-term teratoma tissue (30 weeks in the third teratoma assay). Multiple lymphoid aggregates were still present in the teratoma tissue up to 30 weeks after injection of autologous RhiPSCs (left panel). In the follicles, both CD20-positive B cells (middle panel, detail inset 400×) and CD3-positive T cells (right panel) were present. On high power, T cells are seen scattered throughout the mass (insets, right panel, 400×). All images are H&E, and the magnification is 20× unless otherwise indicated. See also Figures S6 and S7.

process was at least 20-fold less efficient on a per cell basis compared to teratoma formation following simultaneous injection of the same cells into NSG mice. The reduced tumor growth could be hypothesized to be due to a less hospitable microenvironment at rhesus versus murine injection sites based on vascular supply or other factors; however, one would perhaps expect that in the homologous species factors such as cytokines would be more favorable for the growth of RhiPSCs in a macaque as compared to a mouse. However, the more likely issue is the influence of an intact immune system and inflammatory responses. All the teratomas and masses that did result from implantation of autologous RhiPSCs grew more slowly than in NSG mice and seemed to plateau in growth after several weeks, correlating with development of a significant inflammatory infiltrate surrounding the ectopic tissues. None of the cells implanted in NSG mice ever presented with a similar infiltrate, making it unlikely that these lymphoid and myeloid cells originated from the RhiPSCs themselves, although we cannot formally exclude that possibility given that perhaps the murine environment may not support rhesus lymphopoiesis, and development of human hematopoietic cells from human iPSCs within teratomas grown in immunodeficient mice has been reported, albeit only with coinjection of stromal cells optimized for support of hematopoiesis (Amabile et al., 2013). All RhiPSC lines were karyotypically normal when they were transplanted into the autologous animal, although development of a ''neoantigen'' via mutation cannot be ruled out. Sites injected with matrix but without cells, with autologous fibroblasts in matrix, or with RhiPSC-SCs derived from the same iPSC clones in either a plasma clot or a ceramic matrix for the bone formation assays did not show similar inflammatory reactions or immune cell infiltration.

In this study, we transplanted undifferentiated RhiPSCs and differentiated cells derived from the same RhiPSC clones in the same recipient. We observed significant lymphocytic infiltrations in teratoma tissues derived from undifferentiated RhiPSCs, whereas no evidence of lymphocytic infiltrations in bone tissues derived from RhiPSC-SCs. Although previous studies using murine models resulted in conflicting conclusions on the difference of immunogenicity between undifferentiated ESCs and iPSCs, they all described some but various levels of immune responses in teratoma tissues derived from syngenic undifferentiated iPSCs (Araki et al., 2013; Guha et al., 2013; Zhao et al., 2011). Guha et al. observed some lymphocytic infiltrates in teratoma tissues derived from syngenic murine iPSCs and ESCs, but not in in vivo grafts derived from their differentiated counterparts (Guha et al., 2013), which is similar to our results. However, BMSCs potentially have potent anti-inflammatory capabilities (Atoui and Chiu, 2012; Nasef et al., 2008), and therefore reduced inflammation in the bone assay may reflect anti-inflammatory properties of the specific injected iPSC-SCs and may not be generalizable. It is interesting to consider that mixing iPSC-SCs with other iPSC-derived tissues might prevent inflammation and rejection following transplantation of therapeutic tissue grafts. On the other hand, autologous skin fibroblasts cultured in iPSC culture medium as well as on Synthemax II-SC plates did not result in inflammation. Therefore, it seems to be likely that the inflammatory response in the iPSC-derived teratoma tissues is directed against cellular components. Further study will be needed to investigate whether undifferentiated iPSCs and/or tissues derived from them were directly associated with inflammatory reactions observed.

This phenomenon might be due to residual pluripotent gene expression in the tumors derived from autologous iPSCs, as described (Dhodapkar et al., 2010; Tang et al., 2013). However, we did not detect residual OCT4 expression in teratoma tissues despite ongoing lymphocytic infiltration. It is also possible that NK-mediated rejection of PSCs but not of differentiated cells occurred due to low MHC class I expression on PSCs (Atoui and Chiu, 2012; Tang et al., 2013). In this study, we also found that MHC class I was not expressed on undifferentiated RhiPSCs, but was re-expressed during differentiation to RhiPSC-SCs. However, we did not actually detect any significant NK infiltrate in or around the teratomas or fibrous nodules in the autologous macaques, with only a few CD56-positive cells at 2, 5, 10, or 30 weeks. One prior study actually noted a more significant inflammatory response and T cell infiltration after injection of murine iPSCs that did not have full pluripotency in a blastocyst injection assay, suggesting there might be a link between less than complete pluripotency and immunogenicity (Araki et al., 2013). The five clones we used in this study fulfilled all criteria for pluripotency except generating chimeric animals, which is not feasible to perform conventionally in a nonhuman primate model. Also, bone tissues derived from implantation of iPSC-derived stromal cells generated from the same iPSC clones did not exhibited significant T cell infiltration. Further study will be needed to define more specific immune cell types in teratomas, via phenotypic and functional analyses.

iPSC-derived SCs seem to be promising for musculoskeletal regeneration. Potentially, iPSC-SCs can also be used for a variety of other clinical applications including immunomodulation. Recently, derivation of mesenchymal-like precursors and/or subsequent osteoblast lineage cells from human PSCs has been reported (Kuznetsov et al., 2011; Lian et al., 2010; Marolt et al., 2012; Vodyanik et al., 2010). Villa-Diaz et al. showed that human iPSC-derived osteogenic cells contributed to de novo bone formation in calvarial defects produced in immunodeficient mice (Villa-Diaz et al., 2012). Bilousova et al. recently showed that iPSC-derived osteoblasts are able to form bone in syngenic mice (Bilousova et al., 2011). In our model, RhiPSC-SCs morphologically resembled BMSCs, expressed similar cell surface markers, and differentiated down the osteogenic lineage in vitro. However, in vitro osteogenic differentiation from BMSCs has not been a reliable predictor for the functionality of these cells in vivo (Robey, 2011). The heterotopic bone formation assay has been used as a gold standard to investigate the in vivo bone formation ability of human or mouse BMSCs in SCID mice (Kuznetsov et al., 2011; Marolt et al., 2012). In order to circumvent the long term in vitro osteoblast differentiation procedure, we show that RhiPSC-SCs can directly contribute to bone formation in vivo. We show here that these cells are functional in vivo in a clinically relevant autologous setting. One can simultaneously test multiple potential therapeutic cell lines or carriers with a minimum number of animals. Moreover, this assay can be performed simultaneously with a teratoma assay, which allows direct comparison of undifferentiated RhiPSCs and their differentiated progeny in terms of in vivo safety and function. Using this platform, we showed that RhiPS-SCs can produce mineralized bone in vivo. Importantly, in contrast to previous reports using bone differentiation-induced pluripotent cells in mouse models (Hayashi et al., 2012; Kuznetsov et al., 2011), we did not observe any teratoma structures in the tissues derived from RhiPSC-SCs.

In conclusion, by creating and functionally testing iPSC-derived cells in vivo, our model accelerates the potential of iPSC-based cellular therapies. The fact that none of the RhiPSC-SC implants showed any signs of tumor formation, and the low efficiency of teratomas derived from parental iPSCs indicates that the risk of these adverse events is calculable and probably can be further reduced by improved differentiation methods or safety switches such as suicide-gene technology. In summary, we believe that the presented nonhuman primate model will be very valuable for evaluating a wide variety of iPSC-based treatment modalities.

EXPERIMENTAL PROCEDURES

Animals

All animals used in this study were housed and handled in accordance with protocols approved by the Animal Care and Use Committee of the National Heart, Lung and Blood Institute (H-0255 and H-0084).

Generation of Rhesus iPSCs

Rhesus macaque (*Macaca mulatta*) dermal fibroblasts, BMSCs, or $CD34^+$ cells were transduced once with a polycistronic lentiviral vector encoding the four reprogramming factors *OCT4*, *SOX2*, *KLF4*, and *MYC* flanked by loxP sites (Sommer et al., 2010). After 4–5 days, transduced cells were transferred to plates coated with mouse embryonic fibroblasts (MEF) and cultured in 5% oxygen in RhiPSCs medium (KO/DMEM [Gibco, Life Technologies]) supplemented with 20% knockout serum replacement [Life Technologies], 20 ng/ml human bFGF [PeproTech], 0.1 mM MEM nonessential amino acids [Life Technologies], 1% penicillin-streptomycin-glutamine [PSG, Life Technologies], and 0.1 mM 2-mercaptoethanol [Sigma-Aldrich]). Between days 14 and 30, morphologically ESC-like colonies were mechanically selected, transferred to new MEF-coated plates, and mechanically passaged every 4–5 days. Matrigel (BD Biosciences) and Synthemax II-SC (Corning)-coated plates were prepared according to manufacturers' protocols. Clones confirmed to be pluripotent, as described below, were adapted to growth on Matrigel or Synthemax II-SC-coated plates and cultured at least 3 months without obvious phenotypical alterations. Cells were cryopreserved in ES-defined FBS (HyClone) supplemented with 10% DMSO (Sigma-Aldrich). A rhesus macaque ESC line (ORMES-22, a gift from Dr. Shoukhrat Mitalipov) was cultured as described previously (Mitalipov et al., 2006).

Cre-Mediated Transgene Excision

RhiPSCs were cultured on Matrigel-coated 12-well plates in MEF-conditioned medium supplemented with 10 μM Rock inhibitor (STEMCELL Technologies). The following day, a Cre-GFP-puro plasmid (kind gift from Dr. Harry L. Malech) was transfected into the RhiPSCs using Lipofectamine LTX (Invitrogen, Life Technologies) (Merling et al., 2013). Selection was performed with 2–3 μg/ml puromycin for 3 days. MEF feeder cells were added, and medium was changed to RhiPSCs culture medium until the RhiPSCs formed colonies. Removal of the loxP-flanked STEMCCA-loxP vector was confirmed by transgene PCR and copy number qPCR. For further details, please refer to Supplemental Experimental Procedures.

Immunohistochemistry for Pluripotency Markers

Cells were fixed with 4% paraformaldehyde at room temperature for 20 min and blocked with 10% goat or donkey serum (Jackson ImmunoResearch Laboratories). For cytoplasmic protein staining, 0.1% Triton X-100 was added for permeabilization. Primary antibodies were then added and incubated at 4°C overnight. Cells were washed and exposed to secondary antibodies conjugated with fluorochromes before costaining with DAPI. All antibodies are listed in Table S4.

Teratoma Assay in NSG Mice

Female or male immunodeficient NSG mice aged 4–8 weeks were used. Undifferentiated RhiPSCs were harvested, mixed with Matrigel in a 1:1 ratio, or suspended in a rhesus plasma clot (see below) and injected in a volume of 200–300 μl subcutaneously or 100 μl intramuscularly. Mice with tumors with an approximate diameter of 2 cm were euthanized and the excised tumors were fixed in Bouin's solution (Sigma-Aldrich).

SC Differentiation from RhiPSCs

Our differentiation protocol for RhiPSCs toward mesodermal stromal-like cells was adopted and modified from a previous report utilizing human iPSCs (Lian et al., 2010). Briefly, RhiPSCs were cultured on MEF or Matrigel. Undifferentiated RhiPSCs at day 5 were dissociated using Accutase (STEMCELL Technologies), and, if MEF were present, they were removed using magnetic activated cell sorting (Feeder removal kit, Miltenyi Biotec). Cells were transferred onto gelatin-coated plates in BMSC culture medium (a-MEM [Life Technologies], 20% non-heat-inactivated fetal bovine serum [Atlanta Biologicals], and 1% PSG) (Kuznetsov et al., 1997) supplemented with 10 ng/ml bFGF, 10 ng/ml PDGF, and 10 ng/ml EGF, all from PeproTech. After 7–10 days culture, cells were stained with anti-CD73-PE (BD Biosciences) and enriched for CD73-expressing cells using anti-PE magnetic beads (Miltenyi Biotec). Flow cytometric analysis was performed for the following surface antigens: CD44, CD73, CD90, CD105, CD166, CD34, and CD45 (sources listed in Table S4).

For osteogenic differentiation, RhiPSC-SCs were plated at 45,000 cells per 35 mm dish. At 70%–80% confluency, the medium was switched to StemMACS OsteoDiff Medium (Miltenyi Biotec) and changed every 3 days. After 10–14 days, cells were fixed and stained for alkaline phosphates using the SIGMAFAST BCIP/NBT kit (Sigma-Aldrich).

Rhesus Cell In Vivo Transplantation

All procedures were performed under general anesthesia. For teratoma assays, RhiPSCs (5×10^5–2×10^7) were suspended in 270 μl autologous plasma separated from rhesus whole blood anticoagulated with buffered sodium citrate at a final concentration of 0.129 M (BD Biosciences). Clot formation was initiated by addition of $CaCl_2$ to a final concentration of 3 mM, and the solution was immediately injected subcutaneously using 20 gauge needles. For in vivo bone formation assays, a 1–2 cm skin incision was made to create a subcutaneous pocket and an aliquot of 40 mg sterile HA/TCP scaffold ceramic powder (0.5–1.0 mm in diameter, Zimmer) mixed with 2×10^6 autologous RhiPSC-SCs or RhBMSCs was placed in the pocket using a sterile spatula. The incision was closed, and the location of each injection site or bone formation pocket was marked on the skin with a permanent tattoo. Injection sites were assessed in anesthetized animals manually and by ultrasound at least weekly, measured with calipers, and harvested at defined time points. Teratomas were fixed with Bouin's solution and processed for immunohistologic and morphologic analyses. HA/TCP bone explants were fixed, decalcified, processed for histology, and analyzed as previously described (Kuznetsov et al., 2011).

Histological Analyses of Tissue Grafts

Immunohistochemistry studies were performed on 3 μm fixed, paraffin-embedded or frozen tissue sections. The dewaxed and rehydrated slides were subjected to antigen retrieval, consisting of 20 min high temperature heating in PT Link (Dako) in either high pH solution (Dako) for CD3 slides or low pH solution (Dako) for CD20 slides. A microwave retrieval method using a pressure cooker with either 10 mM Citrate buffer (pH 6.0) (K.D. Medical) or 0.5 mM EDTA (pH 8.0) (Quality Biological) was used for CD4 and CD56, respectively. Next, 15 min blocking with 3% Tris goat serum and then incubation with primary antibodies was performed. For detection, the EnVision FLEX mouse kit (Dako) was used for CD3, CD4, and CD20, and the Ultra-View DAB detection kit (Ventana Medical Systems) was used for CD56. Human tonsil sections were included as positive controls for antibody staining. CD8 staining was performed in New England Primate Research Center in Harvard Medical School. Briefly, slides were baked at 60°C, and then a pressure cooker with Trilogy solution (Cell MarqueCA) and Dual Endogenous Enzyme Blocking Reagent (Dako) was used for antigen retrieval and blocking procedures, respectively. For detection, EnVisionTM Dual Link System-HRP kit (Dako) was used. OCT4 staining was performed according to manufacturers' protocols. The detailed information of antibodies used in this study is listed in Table S4.

SUPPLEMENTAL INFORMATION

Supplemental Information includes Supplemental Experimental Procedures, seven figures, and five tables and can be found with this article online at http://dx.doi.org/10.1016/j.celrep.2014.04.019.

AUTHOR CONTRIBUTIONS

S.H., T.W., C.W., V.G., S.P., and A.N. performed and analyzed experiments. S.H., T.W., and C.E.D. wrote the paper. C.E.D., S.H., and T.W. designed the experiments. R.E.D., M.E.M., and S.D.P. transplanted the macaques. N.U. produced reprogramming viruses. S.A.K., T.K., L.L., and P.G.R. performed bone tissue processing and analysis.

ACKNOWLEDGMENTS

This research was supported by the Divisions of Intramural Research at the National Heart, Lung and Blood Institute, the National Institute of Dental and Craniofacial Research, and the National Center for Regenerative Medicine at the NIH. We thank the NHLBI Pathology core for tissue processing and the NHLBI Primate Facility staff for excellent animal care. The STEMCCA vector was kindly provided by Dr. Gustavo Mostoslavsky. We also thank Dr. Shoukhrat Mitalipov for providing the rhesus ESC line (ORMES-22), Dr. Harry L. Malech for sharing the Cre-GFP-puro plasmid, and Dr. Jichun Chen and Marie Desierto for their assistance in performing the teratoma assays. We are indebted to Zimmer for its gift of HA/TCP.

Received: August 26, 2013
Revised: February 9, 2014
Accepted: April 9, 2014
Published: May 15, 2014

REFERENCES

Amabile, G., Welner, R.S., Nombela-Arrieta, C., D'Alise, A.M., Di Ruscio, A., Ebralidze, A.K., Kraytsberg, Y., Ye, M., Kocher, O., Neuberg, D.S., et al. (2013). In vivo generation of transplantable human hematopoietic cells from induced pluripotent stem cells. Blood *121*, 1255–1264.

Araki, R., Uda, M., Hoki, Y., Sunayama, M., Nakamura, M., Ando, S., Sugiura, M., Ideno, H., Shimada, A., Nifuji, A., and Abe, M. (2013). Negligible immunogenicity of terminally differentiated cells derived from induced pluripotent or embryonic stem cells. Nature *494*, 100–104.

Atoui, R., and Chiu, R.C. (2012). Concise review: immunomodulatory properties of mesenchymal stem cells in cellular transplantation: update, controversies, and unknowns. Stem Cells Transl. Med. *1*, 200–205.

Ben-David, U., Gan, Q.F., Golan-Lev, T., Arora, P., Yanuka, O., Oren, Y.S., Leikin-Frenkel, A., Graf, M., Garippa, R., Boehringer, M., et al. (2013). Selective elimination of human pluripotent stem cells by an oleate synthesis inhibitor discovered in a high-throughput screen. Cell Stem Cell *12*, 167–179.

Bianco, P., Riminucci, M., Gronthos, S., and Robey, P.G. (2001). Bone marrow stromal stem cells: nature, biology, and potential applications. Stem Cells *19*, 180–192.

Bianco, P., Robey, P.G., and Simmons, P.J. (2008). Mesenchymal stem cells: revisiting history, concepts, and assays. Cell Stem Cell *2*, 313–319.

Bilousova, G., Jun, H., King, K.B., De Langhe, S., Chick, W.S., Torchia, E.C., Chow, K.S., Klemm, D.J., Roop, D.R., and Majka, S.M. (2011). Osteoblasts derived from induced pluripotent stem cells form calcified structures in scaffolds both in vitro and in vivo. Stem Cells *29*, 206–216.

Cunningham, J.J., Ulbright, T.M., Pera, M.F., and Looijenga, L.H. (2012). Lessons from human teratomas to guide development of safe stem cell therapies. Nat. Biotechnol. *30*, 849–857.

de Almeida, P.E., Ransohoff, J.D., Nahid, A., and Wu, J.C. (2013). Immunogenicity of pluripotent stem cells and their derivatives. Circ. Res. *112*, 549–561.

Dhodapkar, K.M., Feldman, D., Matthews, P., Radfar, S., Pickering, R., Turkula, S., Zebroski, H., and Dhodapkar, M.V. (2010). Natural immunity to pluripotency antigen OCT4 in humans. Proc. Natl. Acad. Sci. USA *107*, 8718–8723.

Di Stasi, A., Tey, S.K., Dotti, G., Fujita, Y., Kennedy-Nasser, A., Martinez, C., Straathof, K., Liu, E., Durett, A.G., Grilley, B., et al. (2011). Inducible apoptosis as a safety switch for adoptive cell therapy. N. Engl. J. Med. *365*, 1673–1683.

Donahue, R.E., and Dunbar, C.E. (2001). Update on the use of nonhuman primate models for preclinical testing of gene therapy approaches targeting hematopoietic cells. Hum. Gene Ther. *12*, 607–617.

Emborg, M.E., Liu, Y., Xi, J., Zhang, X., Yin, Y., Lu, J., Joers, V., Swanson, C., Holden, J.E., and Zhang, S.C. (2013). Induced pluripotent stem cell-derived neural cells survive and mature in the nonhuman primate brain. Cell Rep. *3*, 646–650.

Guha, P., Morgan, J.W., Mostoslavsky, G., Rodrigues, N.P., and Boyd, A.S. (2013). Lack of immune response to differentiated cells derived from syngeneic induced pluripotent stem cells. Cell Stem Cell *12*, 407–412.

Hayashi, T., Misawa, H., Nakahara, H., Noguchi, H., Yoshida, A., Kobayashi, N., Tanaka, M., and Ozaki, T. (2012). Transplantation of osteogenically differentiated mouse iPS cells for bone repair. Cell Transplant. *21*, 591–600.

Illich, D.J., Demir, N., Stojković, M., Scheer, M., Rothamel, D., Neugebauer, J., Hescheler, J., and Zöller, J.E. (2011). Concise review: induced pluripotent stem cells and lineage reprogramming: prospects for bone regeneration. Stem Cells *29*, 555–563.

Kaneko, S., and Yamanaka, S. (2013). To be immunogenic, or not to be: that's the iPSC question. Cell Stem Cell *12*, 385–386.

Kuznetsov, S.A., Krebsbach, P.H., Satomura, K., Kerr, J., Riminucci, M., Benayahu, D., and Robey, P.G. (1997). Single-colony derived strains of human marrow stromal fibroblasts form bone after transplantation in vivo. J. Bone Miner. Res. *12*, 1335–1347.

Kuznetsov, S.A., Cherman, N., and Robey, P.G. (2011). In vivo bone formation by progeny of human embryonic stem cells. Stem Cells Dev. *20*, 269–287.

Lackner, A.A., and Veazey, R.S. (2007). Current concepts in AIDS pathogenesis: insights from the SIV/macaque model. Annu. Rev. Med. *58*, 461–476.

Lee, A.S., Tang, C., Rao, M.S., Weissman, I.L., and Wu, J.C. (2013). Tumorigenicity as a clinical hurdle for pluripotent stem cell therapies. Nat. Med. *19*, 998–1004.

Lian, Q., Zhang, Y., Zhang, J., Zhang, H.K., Wu, X., Zhang, Y., Lam, F.F., Kang, S., Xia, J.C., Lai, W.H., et al. (2010). Functional mesenchymal stem cells derived from human induced pluripotent stem cells attenuate limb ischemia in mice. Circulation *121*, 1113–1123.

Lindsay, R.M., Raisman, G., and Seeley, P.J. (1987). Intracerebral transplantation of cultured neurons after reaggregation in a plasma clot. Neuroscience *21*, 685–698.

Liu, H., Zhu, F., Yong, J., Zhang, P., Hou, P., Li, H., Jiang, W., Cai, J., Liu, M., Cui, K., et al. (2008). Generation of induced pluripotent stem cells from adult rhesus monkey fibroblasts. Cell Stem Cell *3*, 587–590.

Marolt, D., Campos, I.M., Bhumiratana, S., Koren, A., Petridis, P., Zhang, G., Spitalnik, P.F., Grayson, W.L., and Vunjak-Novakovic, G. (2012). Engineering bone tissue from human embryonic stem cells. Proc. Natl. Acad. Sci. USA *109*, 8705–8709.

Merling, R.K., Sweeney, C.L., Choi, U., De Ravin, S.S., Myers, T.G., Otaizo-Carrasquero, F., Pan, J., Linton, G., Chen, L., Koontz, S., et al. (2013). Transgene-free iPSCs generated from small volume peripheral blood nonmobilized CD34+ cells. Blood *121*, e98–e107.

Mitalipov, S., Kuo, H.C., Byrne, J., Clepper, L., Meisner, L., Johnson, J., Zeier, R., and Wolf, D. (2006). Isolation and characterization of novel rhesus monkey embryonic stem cell lines. Stem Cells *24*, 2177–2186.

Nasef, A., Ashammakhi, N., and Fouillard, L. (2008). Immunomodulatory effect of mesenchymal stromal cells: possible mechanisms. Regen. Med. *3*, 531–546.

Okita, K., and Yamanaka, S. (2006). Intracellular signaling pathways regulating pluripotency of embryonic stem cells. Curr. Stem Cell Res. Ther. *1*, 103–111.

Picker, L.J., Hansen, S.G., and Lifson, J.D. (2012). New paradigms for HIV/AIDS vaccine development. Annu. Rev. Med. *63*, 95–111.

Prokhorova, T.A., Harkness, L.M., Frandsen, U., Ditzel, N., Schrøder, H.D., Burns, J.S., and Kassem, M. (2009). Teratoma formation by human embryonic stem cells is site dependent and enhanced by the presence of Matrigel. Stem Cells Dev. *18*, 47–54.

Quarto, R., Mastrogiacomo, M., Cancedda, R., Kutepov, S.M., Mukhachev, V., Lavroukov, A., Kon, E., and Marcacci, M. (2001). Repair of large bone defects with the use of autologous bone marrow stromal cells. N. Engl. J. Med. *344*, 385–386.

Rao, M. (2004). Conserved and divergent paths that regulate self-renewal in mouse and human embryonic stem cells. Dev. Biol. *275*, 269–286.

Robey, P.G. (2011). Cell sources for bone regeneration: the good, the bad, and the ugly (but promising). Tissue Eng. Part B Rev. *17*, 423–430.

Roobrouck, V.D., Ulloa-Montoya, F., and Verfaillie, C.M. (2008). Self-renewal and differentiation capacity of young and aged stem cells. Exp. Cell Res. *314*, 1937–1944.

Schnerch, A., Cerdan, C., and Bhatia, M. (2010). Distinguishing between mouse and human pluripotent stem cell regulation: the best laid plans of mice and men. Stem Cells *28*, 419–430.

Seok, J., Warren, H.S., Cuenca, A.G., Mindrinos, M.N., Baker, H.V., Xu, W., Richards, D.R., McDonald-Smith, G.P., Gao, H., Hennessy, L., et al.; Inflammation and Host Response to Injury, Large Scale Collaborative Research Program (2013). Genomic responses in mouse models poorly mimic human inflammatory diseases. Proc. Natl. Acad. Sci. USA *110*, 3507–3512.

Sommer, C.A., Sommer, A.G., Longmire, T.A., Christodoulou, C., Thomas, D.D., Gostissa, M., Alt, F.W., Murphy, G.J., Kotton, D.N., and Mostoslavsky, G. (2010). Excision of reprogramming transgenes improves the differentiation potential of iPS cells generated with a single excisable vector. Stem Cells *28*, 64–74.

Steinert, A.F., Rackwitz, L., Gilbert, F., Nöth, U., and Tuan, R.S. (2012). Concise review: the clinical application of mesenchymal stem cells for musculoskeletal regeneration: current status and perspectives. Stem Cells Transl. Med. *1*, 237–247.

Tang, C., Lee, A.S., Volkmer, J.P., Sahoo, D., Nag, D., Mosley, A.R., Inlay, M.A., Ardehali, R., Chavez, S.L., Pera, R.R., et al. (2011). An antibody against SSEA-5 glycan on human pluripotent stem cells enables removal of teratoma-forming cells. Nat. Biotechnol. *29*, 829–834.

Tang, C., Weissman, I.L., and Drukker, M. (2013). Immunogenicity of in vitro maintained and matured populations: potential barriers to engraftment of human pluripotent stem cell derivatives. Methods Mol. Biol. *1029*, 17–31.

Tesar, P.J., Chenoweth, J.G., Brook, F.A., Davies, T.J., Evans, E.P., Mack, D.L., Gardner, R.L., and McKay, R.D. (2007). New cell lines from mouse epiblast share defining features with human embryonic stem cells. Nature *448*, 196–199.

Villa-Diaz, L.G., Brown, S.E., Liu, Y., Ross, A.M., Lahann, J., Parent, J.M., and Krebsbach, P.H. (2012). Derivation of mesenchymal stem cells from human induced pluripotent stem cells cultured on synthetic substrates. Stem Cells *30*, 1174–1181.

Vodyanik, M.A., Yu, J., Zhang, X., Tian, S., Stewart, R., Thomson, J.A., and Slukvin, I.I. (2010). A mesoderm-derived precursor for mesenchymal stem and endothelial cells. Cell Stem Cell *7*, 718–729.

Wu, C., Jares, A., Winkler, T., Xie, J., Metais, J.Y., and Dunbar, C.E. (2013). High efficiency restriction enzyme-free linear amplification-mediated polymerase chain reaction approach for tracking lentiviral integration sites does not abrogate retrieval bias. Hum. Gene Ther. *24*, 38–47.

Zhao, T., Zhang, Z.N., Rong, Z., and Xu, Y. (2011). Immunogenicity of induced pluripotent stem cells. Nature *474*, 212–215.

Zhong, B., Watts, K.L., Gori, J.L., Wohlfahrt, M.E., Enssle, J., Adair, J.E., and Kiem, H.P. (2011). Safeguarding nonhuman primate iPS cells with suicide genes. Mol. Ther. *19*, 1667–1675.